THE STRUCTURE OF LINDGRENITE

L. D. CALVERT[1] AND W. H. BARNES

Division of Pure Physics, National Research Council, Ottawa, Canada

ABSTRACT

Two-dimensional Patterson, Fourier and difference syntheses have been used to solve and refine the structure of lindgrenite, $2CuMoO_4.Cu(OH)_2$. The results show an infinite three-dimensional network of $CuO_4(OH)_2$ octahedra sharing edges to form endless chains which are cross-linked through MoO_4 tetrahedra sharing corners with adjacent octahedra. Powder data (indexed for $d \geqslant 2.25$ Å) are given in an Appendix as an aid to the identification of lindgrenite.

Introduction

Lindgrenite, $2CuMoO_4.Cu(OH)_2$, is a comparatively rare mineral originally found in Chile, and first described by Palache (1935). It has more recently been identified in Idaho and in Arizona (Cannon & Grimaldi, 1953), and in Great Britain (Kingsbury & Hartley, 1954). Lindgrenite is monoclinic; its unit cell constants have been reported as $a = 5.61_3$ Å, $b = 14.03$ Å, $c = 5.40_5$ Å, $\beta = 98°23'$, with two formula units per cell, and space group $P2_1/n$ (Barnes, 1949). Its structure is of interest as that of a naturally occurring molybdate, of which few are known, and also as that of an oxy-hydroxy copper compound.

Experimental

A portion of the original specimen studied by Palache (1935) and by Barnes (1949) was available through the kindness of Professor Clifford Frondel. Two crystals from this specimen were employed in the present investigation. The first was cut from a large plate and had dimensions of $80 \times 90 \times 110$ μ. The $hk0$ and $0kl$ reflections were recorded on precession photographs (Mo$K\alpha$ radiation, $\lambda = 0.7107$ Å) from some of which the unit cell constants and the space group, reported previously (Barnes, 1949), were confirmed. The measurements on those precession films ($\bar{\mu} = 30°$) from which the values of a, b and c were calculated, utilized the row lines of spots from the resolved α_1 ($\lambda = 0.70926$ Å), α_2 ($\lambda = 0.71354$ Å) doublet. Weissenberg photographs (Cu$K\alpha$ radiation, $\lambda = 1.5418$ Å) were employed for the $\{h0l\}$ zone. The intensities of the spots on the precession films were estimated by comparison with a scale obtained by means of a rotating sector, while a logarithmic-interval scale

[1]National Research Laboratories Postdoctorate Fellow, now with Division of Applied Chemistry, National Research Council, Ottawa, Canada.

prepared from the crystal itself was used for the Weissenberg films. All intensities were corrected as usual for Lorentz and polarization factors (Buerger, 1941; Waser, 1951). Absorption corrections, however, were not applied to the data from the precession photographs ($\bar{\mu} = 25°$) because they are virtually constant for Mo radiation over the observed range of $\sin\theta$, but it was necessary to correct the intensities of the $h0l$ reflections (Cu radiation) and an approximate analytical method was adopted. The relative values of $|F|^2$ were placed on an absolute scale by the procedure of Wilson (1942).

After a few stages of refinement of a trial structure, however, it became clear that observed structure amplitudes of greater accuracy would be necessary in order to establish the co-ordinates of the oxygen atoms with any degree of certainty. For this purpose a second crystal was reduced to a sphere of radius $98 \pm 1\ \mu$ in a Bond (1951) Sphere Grinder, although some difficulty was experienced at first owing to the pronounced cleavage parallel to (010). The spherical crystal was finally obtained as follows. Several fragments were ground against 325 grit aluminium oxide paper, under an air pressure of 10 to 15 pounds per square inch, until roughly spherical particles were produced. These particles were then ground individually in short stages of about 1 minute each using 600 grit silicon carbide paper and an air pressure of 5 p.s.i., because tests had shown that continued treatment under the initial conditions caused the crystals to shatter. At the end of each stage the particle was examined under a stereoscopic microscope. After several attempts a satisfactory sphere, free from visible cracks or partings, was obtained.

The reflections from the $\{hk0\}$ zone of the spherical crystal were recorded with Cu$K\alpha$ radiation in an integrating Weissenberg instrument (Wiebenga & Smits, 1950). The strong and medium intensities were measured with a divided-beam photometer. Long-exposure non-integrated photographs were employed for recording the weak reflections, the intensities of which were estimated by careful comparison with a photographic intensity scale prepared from the same crystal. The intensities of each of the four types of equivalent reflections, $hk0$, $h\bar{k}0$, $\bar{h}k0$, $\bar{h}\bar{k}0$, were measured and the mean of the results for each set of four equivalent planes was adopted, because in some cases (large $\sin\theta$) the observed values within each set were not exactly equal. Of 100 possible reflections from this zone, 99 were observed. The intensities of 58 were measured with the photometer, the intensities of 13 were estimated by eye with the aid of the intensity scale, and the intensities of 28 of medium strength were obtained by both methods to provide correlation between the results from the photometer and those from the eye estimations.

The reflections from the $\{h0l\}$ and $\{0kl\}$ zones were recorded on

precession photographs taken with $\bar{\mu} = 30°$ and Mo$K\alpha$ radiation. Twelve films were exposed for various pre-determined times from $\frac{1}{2}$ hour to 116 hours for the $\{h0l\}$ zone, and ten films with exposure times of $\frac{1}{2}$ hour to 129 hours were obtained for the $\{0kl\}$ zone. All but one of the 48 possible reflections from $\{h0l\}$, and all 122 possible reflections from $\{0kl\}$, were observed. The structure amplitudes of 5 of the former (including the one unobserved), and 14 of the latter, were not included in the refinement calculations because of uncertainty in the Lorentz-polarization corrections at the large $\sin\theta$ values involved.

For estimating the intensities of the reflections from these two zones, a scale was prepared from a set of precession photographs, available in the laboratory, which had been taken with timed exposures, in the ratio 1:2:4:8:16:32:64, of a zone of another mineral. The spot due to a specific reflection was selected on the basis of its photographic density on the film of shortest exposure time and its very close similarity in size and shape to those on the lindgrenite films, and a strip containing it was cut from each of the seven films. The intensities of all reflections from the $\{h0l\}$ and $\{0kl\}$ zones of lindgrenite were estimated by direct comparison with this exposure scale according to the usual multiple exposure technique, and the results were arranged in order of increasing intensity for each zone. This order and the numerical values in each list were then refined by careful visual comparison of adjacent entries with the corresponding spots on the appropriate set of lindgrenite films. This procedure is equivalent to the use of much smaller interpolation intervals than normally is feasible with a graded intensity scale alone; it was particularly desirable in the present case because of the rather coarse scale employed for the initial estimations. The intensities of all reflections were measured, including those from equivalent planes (i.e., $(h0l)$, $(\bar{h}0\bar{l})$ in $\{h0l\}$; $(0kl)$, $(0\bar{k}l)$, $(0k\bar{l})$, $(0\bar{k}\bar{l})$ in $\{0kl\}$). The average value for each set of equivalent reflections was accepted in all cases.

The observed intensities for each of the three axial zones were corrected for Lorentz-polarization effects, appropriate absorption corrections for a spherical crystal (Taylor, 1944; Evans & Ekstein, 1952) were applied, and the final values of $|F|^2$ were placed on an absolute sale by Wilson's method. It is of interest to note that the discrepancy, $\Sigma|F_1-F_2|/\Sigma|F_1|$, between the structure amplitudes, $|F_1|$, for the spherical crystal, and those, $|F_2|$, for the non-spherical crystal, is 0.09, indicating systematic improvement even when allowance is made for random variations.

Trial Structure; Patterson Synthesis

The co-ordinates of the equivalent positions in the space group $P2_1/n$ (C_{2h}^5), unique axis b, are

(a) 000; $\frac{1}{2}\frac{1}{2}\frac{1}{2}$ (b) $\frac{1}{2}00$; $0\frac{1}{2}\frac{1}{2}$
(c) $0\frac{1}{2}0$; $\frac{1}{2}0\frac{1}{2}$ (d) $\frac{1}{2}\frac{1}{2}0$; $00\frac{1}{2}$
(e) xyz; $\frac{1}{2}+x$, $\frac{1}{2}-y$, $\frac{1}{2}+z$; $\overline{xyz}$; $\frac{1}{2}-x$, $\frac{1}{2}+y$, $\frac{1}{2}-z$.

The unit cell of lindgrenite contains 6 copper atoms and 4 molybdenum atoms. It is necessary, therefore, to place at least two of the former in one of the four sets of two-fold special positions. Since these differ only in choice of origin, two atoms (designated Cu_1) may be assigned to (a) with co-ordinates 0, 0, 0 and $\frac{1}{2}$, $\frac{1}{2}$, $\frac{1}{2}$. There remain four atoms of copper (designated Cu_2) and four atoms of molybdenum which may be expected to occupy two sets of general positions (e). It is only necessary, therefore, to determine the co-ordinates of one Cu_2 and one Mo in order to establish the sites of all the metal atoms. An examination of the morphology, optical characteristics, and observed structure amplitudes revealed no features of direct assistance in suggesting possible locations for these metal atoms or for the oxygen atoms.

Patterson projections on (100), (010), and (001) were calculated and are shown in Fig. 1.[2] It may be noted that the majority of the peaks, with the exception of that at the origin, are approximately equal in height, and that there is remarkably good resolution in the (010) pro-

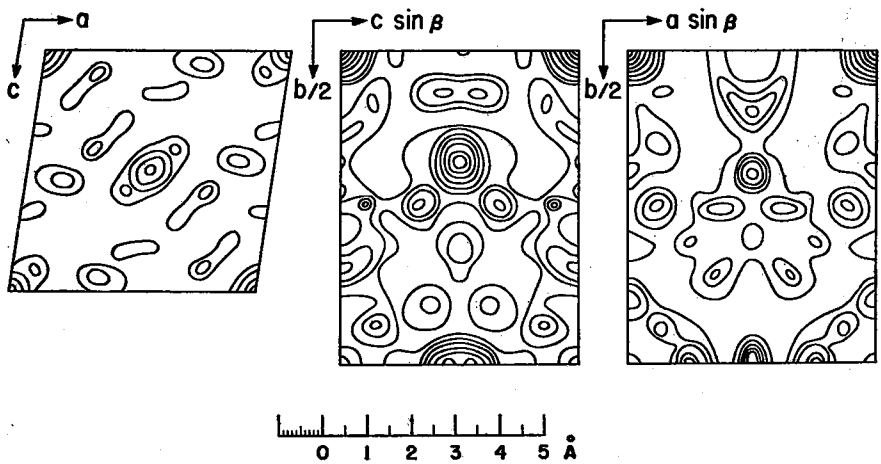

FIG. 1. Patterson maps for the {$h0l$}, {$0kl$}, and {$hk0$} zones of lindgrenite. Contours at equal, but arbitrary, intervals above an arbitrary base; contour intervals doubled at origin.

[2]While checking the completed drawings for Figs. 1 to 7, an accidental error of about 1% (apparently involving the factor $\sin\beta = 0.9893$) was detected in some of the lengths representing a, c, $a\sin\beta$, $c\sin\beta$. Because the figures are designed primarily for illustrative purposes, and the error is small, it was not considered worthwhile to repeat the laborious plotting and drawing required to prepare a new set of figures.

jection despite the length (14.03 Å) of the b axis. Correlation of the three maps gave a list of maxima in the Patterson unit cell which were readily interpreted as follows.

Because of the large differences between the atomic numbers of copper and molybdenum and that of oxygen it was assumed that only the peaks due to metal–metal interactions would appear on the Patterson maps. The high background level of the projections, therefore, is explicable as representing the large number of unresolved metal–oxygen and oxygen–oxygen vectors.

Now as a consequence of the n glide at $y = \frac{1}{4}$ in space group $P2_1/n$ an atom at x, y, z is paired with another at $\frac{1}{2}+x$, $\frac{1}{2}-y$, $\frac{1}{2}+z$ and it may be expected, therefore, that maxima will appear in the Patterson cell along the line $\frac{1}{2}$, v, $\frac{1}{2}$ with $v = \frac{1}{2}\pm 2y$, and, for convenience, attention may be centred on $v = \frac{1}{2}-2y$. Examination of the (001) Patterson map (Fig. 1) shows three peaks, with $v = 8/120$, $24/120$, $37/120$, for which $0<v<\frac{1}{2}$, along the line $\frac{1}{2}$, v. Two of these must be caused by Cu_2-Cu_2 and Mo−Mo interactions, respectively, but the close similarity among the heights of the three peaks prohibits a direct choice of the appropriate pair. The y co-ordinates of the atoms responsible for the three peaks are 26/120, 18/120, 11/120, respectively. Taking these in pairs, assigning them to metal atoms having scattering powers of $\frac{1}{2}(f_{Cu}+f_{Mo})$, and with Cu_1 at $y = 0$, three sets of structure factors were calculated for the $0k0$ reflections. Reasonable agreement with the observed structure amplitudes was found only with the two composite metal atoms at $y = 18/120$ and 11/120, respectively.

Restricting attention to the atom Cu_1 at 0, 0, 0 and another metal atom (Cu_2 or Mo) in a set of general positions (e), twelve independent Patterson maxima should occur for which the Patterson co-ordinates u, v, w have the following values in terms of the atomic co-ordinates: x, y, z; $\frac{1}{2}+x, \frac{1}{2}-y, \frac{1}{2}+z$; $\frac{1}{2}, \frac{1}{2}+2y, \frac{1}{2}$; $2x, 2y, 2z$; $\frac{1}{2}+2x, \frac{1}{2}, \frac{1}{2}+2z$; $2x, \overline{2y}, 2z$; plus these with changed signs. Since there are two metal atoms in separate groups of general positions, two such groups of maxima, having values of v corresponding to $y = 18/120$ and 11/120, respectively, were sought among the Patterson maps, and all peaks corresponding to both groups were found. From the u, w Patterson co-ordinates of these two maxima, values of x, $z = 104/120$, 56/120 and 52/120, 104/120, associated with $y = 18/120$ and 11/120, respectively, were deduced, and their validity was tested by calculating structure factors for the $h00$ and $00l$ reflections, respectively, as for the $0k0$ reflections, and comparing the results with the observed structure amplitudes.

As a final confirmation of the x, y, z co-ordinates for the two metal atoms in the separate sets of general positions, all other possible inter-

actions among all the metal atoms were calculated and were found to account for the remaining important features of the three Patterson projections. Furthermore, the closest metal–metal distances were reasonable, namely 3.1 to 3.8 Å. It was not possible at this stage, however, to distinguish Cu_2 from Mo.

Refinement; F_o and $(F_o - F_c)$ Syntheses

The Fourier projection on (001) was calculated for Cu_1 atoms in special positions (*a*) at x, $y = 0$, 0 and $\frac{1}{2}$, $\frac{1}{2}$, and for metal atoms, each with scattering power $\frac{1}{2}(f_{Cu}+f_{Mo})$, in two sets of general positions (*e*) for which x, $y = 0.43$, 0.09 and 0.87, 0.15, respectively, as deduced from the Patterson maps. Atomic scattering factors taken from the *Internationale Tabellen* (1935) were used throughout the structure study because the substitution of approximate ionic scattering factors (Cu^{2+}, Mo^{6+}) in the later stages of refinement caused no significant changes in the discrepancy factor, R. The atomic scattering factors were corrected for dispersion by the formula of Hönl (1933), and were modified by a temperature factor with $B = 1.0$ derived from the Wilson plot with which the observed intensities were scaled. Only those planes whose signs had been established by the calculated structure factors were included in the Fourier synthesis. The discrepancy factor, R, was 0.57, taking $|F_o| = 0$ for all unobserved reflections. In addition to several peaks of about 10 *e.* $Å^{-2}$, the Fourier map showed two large peaks of heights 30 *e.* $Å^{-2}$ and 50 *e.* $Å^{-2}$ which were assigned to the Cu_2 and Mo atoms, respectively.

On the basis of the x, y co-ordinates for Cu_2 and Mo derived from this Fourier map, together with those for Cu_1, a difference synthesis was computed for which $R = 0.43$. Three peaks were well resolved in the difference map and were assumed to represent oxygen atoms. Metal atom shifts were calculated from the gradients (Cruickshank, 1949), and structure factors were recalculated with the revised metal co-ordinates and those of the three oyxgen atoms. The scale of the observed intensities and the value of B for the metal atoms were readjusted. For the oxygen atoms B was taken as twice that of the metal atoms on the basis of the relative sharpness of the peaks in the Fourier maps.

A second difference synthesis, with the metal atoms and the three oxygen atoms removed, reduced R to 0.25 and revealed the positions of the two remaining oxygen atoms. Refinement of the atomic positions was effected and adjustment of the scale and temperature factors was again carried out. Because the map showed some disturbing features, however, the next difference synthesis was calculated in two parts, (*a*) with only the metal atoms removed, and (*b*) with all the atoms removed. The

discrepancy factor, $R = 0.22$, was the same in both cases, suggesting that the x, y co-ordinates of one or more of the oxygen atoms must be incorrect. Another difference synthesis, therefore, was calculated with all of the metal and three of the five oxygen atoms removed. The resulting map ($R = 0.25$) revealed new sites for two of the oxygen atoms. Four more difference syntheses brought the shifts in co-ordinates to random values and reduced R to 0.11.

The $\{0kl\}$ zone was independently examined in the same way, starting with a Fourier projection on (100) based on atoms of Cu_I at $y, z = 0, 0$ and $\frac{1}{2}, \frac{1}{2}$, and metal atoms with $f = \frac{1}{2}(f_{Cu}+f_{Mo})$ in two sets of general positions for which $y, z = 0.09, 0.87$ and $0.15, 0.47$, respectively, as deduced from the Patterson maps. The electron density map ($R = 0.34$) showed two peaks of 44 *e.* Å^{-2} and 61 *e.* Å^{-2} with y co-ordinates in agreement with those of the positions assigned to Cu_2 and Mo, respectively, in the (001) Fourier projection. The three highest of the remaining peaks were selected as representing the positions of oxygen atoms.

A difference synthesis, calculated with only the metal atoms removed, reduced R to 0.25, while with all the atoms removed R was 0.19. The highest peak in the second map was identified tentatively as representing a fourth oxygen atom. The next difference synthesis ($R = 0.16$), calculated with the metal atoms and the four oxygen atoms removed, however, indicated that the co-ordinates of one oxygen atom probably were incorrect. This suspicion was confirmed and the correct position of this atom and that of the fifth oxygen atom were revealed in the next difference map ($R = 0.20$). Three more difference syntheses reduced the shifts of atomic positions to random values ($R = 0.15$). The y co-ordinates of all atoms at this stage were in satisfactory agreement with those derived independently from the analysis of the Fourier and difference maps for the $\{hk0\}$ zone. In both zones, $|F_o - F_c|$ for the unobserved reflections was assumed to be 0.7 of the lowest observable $|F_o|$ in the first few difference syntheses, but all unobserved reflections were omitted from the later calculations.

The results for the two zones were combined, but several features of the resulting structure were unsatisfactory, particularly two of the Mo—O and two of the O—O distances. All of these were dependent on the co-ordinates assigned to oxygen atoms which, in both projections, would be affected by the presence of neighbouring metal atoms. Using the co-ordinates derived from these two zones, therefore, a Fourier projection and a difference map were calculated for the $\{h0l\}$ zone. Two oxygen atoms were well resolved but atomic shifts were indicated which suggested the presence of systematic errors in certain of the oxygen atom co-ordinates derived from the $\{hk0\}$ and $\{0kl\}$ zones.

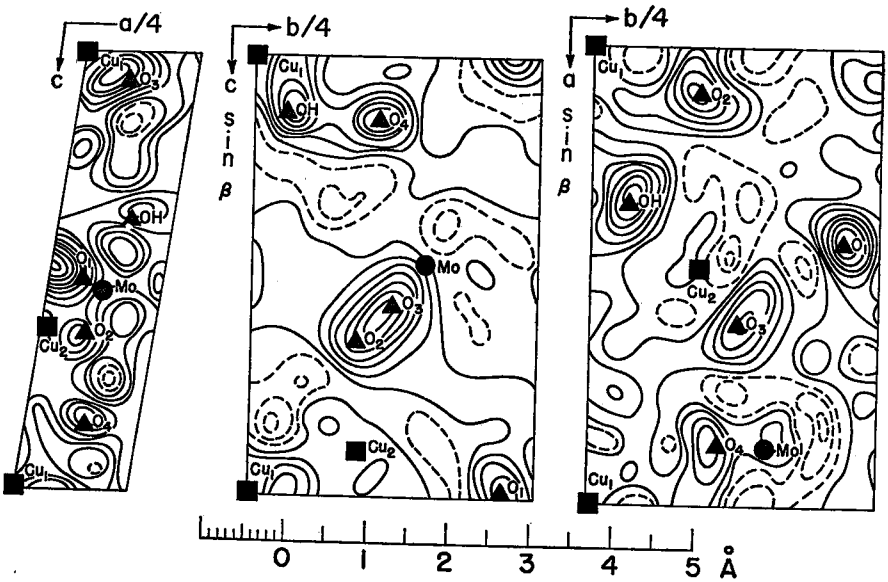

FIG. 2. Final partial difference maps for the $\{h0l\}$, $\{0kl\}$, and $\{hk0\}$ zones of lindgrenite. Metal atoms removed. Contours at intervals of $2e.Å^{-2}$; zero and negative contours broken. Atomic sites labelled.

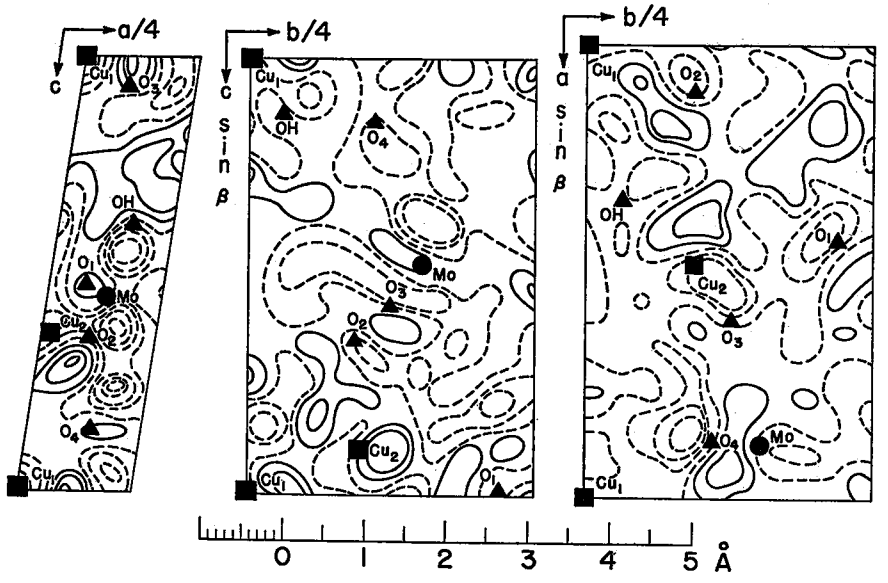

FIG. 3. Final difference maps for the $\{h0l\}$, $\{0kl\}$, and $\{hk0\}$ zones of lindgrenite. All atoms removed. Contours at intervals of $1e.Å^{-2}$; zero and negative contours broken. Atomic sites labelled.

At this stage the spherical crystal was prepared and the more complete and accurate intensity data were collected. Refinement of the three axial zones was resumed with the use of the new structure amplitudes. To reduce the shifts in atomic co-ordinates again to random values, two difference syntheses were required for the (100) projection, and three each for the (001) and (010) projections.

The last partial difference maps (only the metal atoms removed) are shown in Fig. 2 and the corresponding complete difference maps (all atoms removed) are reproduced in Fig. 3. The variations in electron density in the latter are of the order to be expected from random experimental errors, and the gradients are close to zero at all the atomic sites. The absence of any systematic features in the difference maps implies that the final values of the temperature-factor constant B (1.00 for O;

TABLE 1. FRACTIONAL CO-ORDINATES OF THE ATOMS
(Derived Separately for Each Zone; Weighted Means, w. m.; Values for Unresolved Atoms are in Parentheses)

Atom	x			y			z		
	$\{h0l\}$	$\{hk0\}$	w.m.	$\{0kl\}$	$\{hk0\}$	w.m.	$\{0kl\}$	$\{h0l\}$	w.m.
Cu_1	0	0	0	0	0	0	0	0	0
Cu_2	(0.4890)	0.4884	0.4885	0.0939	0.0944	0.0942	0.8644	0.8640	0.8642
Mo	0.8766	0.8771	0.8769	0.1545	0.1543	0.1544	0.4550	0.4555	0.4552
O_1	(0.435)	0.432	0.432	0.222	0.220	0.221	0.977	(0.979)	0.977
O_2	(0.101)	(0.094)	0.096	(0.095)	(0.093)	0.094	(0.641)	(0.646)	0.642
O_3	(0.600)	(0.600)	0.600	(0.130)	0.129	0.130	(0.550)	(0.562)	0.554
O_4	(0.867)	0.866	0.866	(0.114)	(0.108)	0.112	0.144	0.150	0.149
OH	0.344	0.337	0.341	0.032	0.031	0.031	0.120	0.124	0.123

TABLE 2. INTERATOMIC DISTANCES IN Å
($CuO_4(OH)_2$ Octahedra, Shared Edges indicated by Asterisks; MoO_4 Tetrahedron)

	O_2	O_2	O_4	O_4	OH	OH
Cu_1	2.46	2.46	1.96	1.96	1.98	1.98
O_2			3.09	3.18	2.90*	3.40
O_4					2.66*	2.91

	O_1	O_2	O_3	O_4	OH	OH
Cu_2	1.92	2.36	1.93	2.45	1.94	2.00
O_1		3.02	2.89	2.92	2.85	
O_2			2.98		2.90*	3.68
O_3				3.36		2.84
O_4					3.14	2.66*
OH						2.53*

	O_1	O_2	O_3	O_4
Mo	1.77	1.70	1.75	1.75
O_1		2.85	2.87	2.93
O_2			2.80	2.81
O_3				2.82

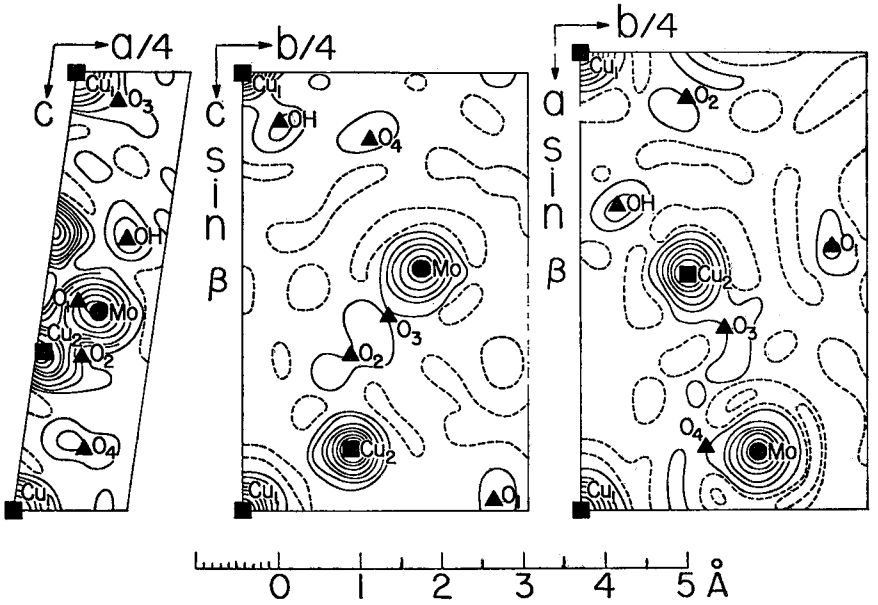

FIG. 4. Final Fourier maps for the $\{h0l\}$, $\{0kl\}$, and $\{hk0\}$ zones of lindgrenite. Contours at intervals of $10e.Å^{-2}$, except $20e.Å^{-2}$ around Mo; zero and negative contours broken.

0.53 for Cu; 0.53 for Mo) are reasonable, although the value adopted for oxygen is much less critical than that used for the metal atoms. There is a slight suggestion of an anisotropic temperature effect associated with Cu_1 at 0, 0 in the (100) map of Fig. 3.

The fractional atomic co-ordinates, each determined from two different zones, are given in Table 1. The interatomic distances, calculated twice (i.e., for each pair of atoms in two different regions of the unit cell), are listed in Table 2. For each co-ordinate the two values derived from the appropriate projections were weighted inversely as the variance (σ^2) of each to give the weighted means shown in Table 1. That the differences between the individual values of the co-ordinates and their weighted means cannot be considered as significant was supported by the results of a χ^2 test (Weatherburn, 1947).

The identification of which oxygen atom must represent the OH group was made as follows. Each Mo is linked to 4O so that, if Mo is assumed to have a formal electrostatic charge of 6+, a Mo—O bond has a value of $1\frac{1}{2}$. Similarly, each Cu, with a charge of 2+, is joined to 6O, thus giving the Cu—O bond a value of $\frac{1}{3}$. Now atoms O_1 and O_3 are each shared between 1 Mo and 1 Cu so that their formal charges of 2− are approximately neutralized ($1\frac{1}{2}+\frac{1}{3}$), and atoms O_2 and O_4 are each linked to

1 Mo and to 2 Cu, thus accounting for their charges ($1\frac{1}{2}+\frac{2}{3}$) also. But O_5 is closely associated only with 3 Cu and thus retains an apparent net formal charge of 1−, unless it does in fact represent the OH group. It has, therefore, been designated OH in the figures and tables.

Electron density projections, calculated with the signs from the final stage of refinement, are presented in Fig. 4. In these Fourier maps, the strongly negative region around the molybdenum atom indicates the magnitude of the effects which caused some of the difficulties in locating the sites of the oxygen atoms.

Accuracy of the Results

The observed structure amplitudes and the calculated structure factors are listed, separately for each of the three axial zones, in Table 3.

For each of the 28 planes in the $\{hk0\}$ zone, the reflection intensities of which were measured both with the photometer (integrated Weissenberg photographs) and by eye (non-integrated Weissenberg photographs), the value of F_o in Table 3 is the mean of the two results. The discrepancy, $\Sigma|F_p-F_e|/\Sigma|F_p|$, between the structure amplitudes, $|F_p|$, from the photometric measurements and those, $|F_e|$, estimated by eye is 0.06_8 when the results for all 28 planes are included. If the (280) plane, for which $|\Delta F|$ is greater than 5 times the probable error of a single ΔF (calculated for all 28 values of $\Delta F = |F_p|-|F_e|$) is rejected (Scarborough, 1950, p. 437), this discrepancy is reduced to 0.06_1. For the other 27 planes, $\overline{\Delta F} = -0.130$, $\Sigma(\Delta F) = -3.5$, $\Sigma(\Delta F)^2 = 56.87$. The estimated standard deviation of ΔF,

$$\sigma(\Delta F) = \sqrt{\left[\Sigma(\Delta F)^2 - \frac{\{\Sigma(\Delta F)\}^2}{n}\right]/(n-1)},$$

is 1.47, and $\sigma(F) = \sqrt{\Sigma(\Delta F)^2/2n} = 1.03$. The e.s.d. of the mean $\Delta F = \sigma(\overline{\Delta F}) = \sigma(\Delta F)/\sqrt{n} = 0.283$, and $\overline{\Delta F}/\sigma(\overline{\Delta F}) = 0.459$. This ratio is less than that (0.684) for the 50% probability level (Youden, 1951), thus demonstrating that there is no significant difference between the results obtained with the photometer and those from the eye estimations. Furthermore, there is no significant difference between the discrepancy factors, $R = \Sigma|F_o-F_c|/\Sigma|F_o|$, calculated with $F_o = F_p$ and with $F_o = F_e$ respectively, for the 27 reflections.

It is of interest that comparable results are obtained by application of the same treatment to the structure amplitudes for dibenzyl, $|F_R|$, obtained by Robertson (1934) from intensities measured with an integrating photometer, and those, $|F_J|$, obtained by Jeffrey (1947) from eye estimations with the aid of a calibrated intensity scale. There are 95 observed reflections (Jeffrey, 1947, p. 224) for which both F_R and F_J are available. Jeffrey points out that the difference between the two

TABLE 3. STRUCTURE FACTOR DATA FOR THE {0*kl*}, {*h*0*l*} AND {*hk*0} ZONES SEPARATELY

0*kl*	$\|F_o\|$	F_c	0*kl*	$\|F_o\|$	F_c	0*kl*	$\|F_o\|$	F_c
002	170.2	+166.7	054	66.9	− 65.1	0.11.1	75.2	+ 75.0
004	8.3	− 7.6	055	38.9	+ 44.4	0.11.2	42.4	− 47.5
006	40.1	+ 41.2	056	54.8	− 49.7	0.11.3	6.5	+ 4.1
011	40.6	+ 36.1	060	38.5	+ 41.0	0.11.4	48.7	− 53.7
012	72.5	+ 70.7	061	19.4	− 15.7	0.11.5	7.1	+ 7.6
013	63.3	− 68.3	062	122.4	+120.9	0.12.0	92.7	+ 94.0
014	60.5	+ 58.0	063	7.0	+ 5.2	0.12.1	36.0	+ 38.4
015	6.0	− 5.2	064	114.0	+107.2	0.12.2	44.2	+ 46.3
016	35.9	+ 33.4	065	42.3	+ 39.9	0.12.3	46.4	+ 47.9
017	58.6	+ 58.6	066	13.5	− 9.1	0.12.4	13.0	+ 5.1
020	65.5	+ 56.2	071	94.9	− 95.5	0.12.5	20.9	+ 13.5
021	38.8	+ 30.6	072	19.8	− 16.8	0.13.1	38.2	− 34.0
022	29.2	− 19.8	073	14.7	− 12.0	0.13.2	36.2	+ 39.1
023	21.7	− 26.4	074	42.4	+ 38.6	0.13.3	12.0	− 7.2
024	28.6	− 26.7	075	15.2	+ 16.7	0.13.4	5.5	− 1.7
025	91.4	− 91.8	076	58.4	+ 54.8	0.13.5	12.0	+ 16.5
026	28.8	+ 27.2	080	73.1	+ 72.0	0.14.0	31.8	+ 29.7
027	47.7	− 42.3	081	97.7	− 96.3	0.14.1	18.9	+ 22.6
031	168.3	+172.4	082	52.3	+ 46.8	0.14.2	51.8	+ 57.5
032	38.8	+ 35.9	083	104.0	−103.9	0.14.3	18.7	− 16.5
033	112.3	+106.1	084	22.9	+ 27.9	0.14.4	53.9	+ 58.5
034	4.7	− 2.3	085	17.9	− 17.4	0.15.1	9.7	+ 12.8
035	35.8	+ 32.4	086	17.5	+ 23.3	0.15.2	50.1	+ 57.1
036	17.0	− 20.9	091	122.2	+129.8	0.15.3	52.8	+ 56.3
037	9.8	− 9.2	092	29.3	− 29.5	0.15.4	36.1	+ 37.0
040	143.0	−144.9	093	44.4	+ 42.5	0.16.0	81.3	− 88.1
041	66.0	+ 65.2	094	41.1	+ 39.8	0.16.1	3.6	+ 3.5
042	14.4	− 16.2	095	19.8	+ 21.9	0.16.2	23.4	− 21.0
043	66.4	+ 65.7	096	58.1	+ 54.9	0.16.3	5.3	− 1.8
044	52.6	+ 49.0	0.10.0	19.1	+ 20.1	0.17.1	32.5	+ 31.8
045	17.0	+ 10.8	0.10.1	23.8	− 22.9	0.17.2	36.1	− 36.2
046	13.4	+ 8.9	0.10.2	45.4	− 44.6	0.17.3	55.1	+ 55.9
047	26.1	+ 21.2	0.10.3	6.8	+ 4.3	0.18.0	15.6	+ 16.5
051	8.8	+ 8.6	0.10.4	50.1	− 49.6	0.18.1	9.7	− 11.7
052	41.0	− 43.7	0.10.5	49.3	+ 49.6	0.18.2	28.3	+ 31.2
053	90.6	+ 87.3	0.10.6	34.7	+ 42.6	0.19.1	19.0	− 17.2

*h*0*l*	$\|F_o\|$	F_c	*h*0*l*	$\|F_o\|$	F_c	*h*0*l*	$\|F_o\|$	F_c
002	151.2	+158.7	402	78.8	− 75.0	$30\bar{3}$	62.5	+ 62.2
004	9.3	− 13.7	404	30.2	− 29.2	$30\bar{5}$	19.7	+ 19.1
006	42.8	+ 39.4	501	41.7	+ 38.5	$30\bar{7}$	64.1	− 59.9
101	87.8	− 82.6	503	51.7	+ 59.6	$40\bar{2}$	5.6	− 4.7
103	92.7	+ 88.7	600	41.1	+ 52.3	$40\bar{4}$	33.2	− 27.2
105	65.8	+ 66.9	602	14.0	+ 16.8	$40\bar{6}$	22.3	+ 25.4
107	25.1	+ 21.4	701	32.5	− 34.8	$50\bar{1}$	35.0	+ 39.7
200	158.5	+153.9	$10\bar{1}$	154.5	−165.7	$50\bar{3}$	108.0	+110.0
202	18.6	− 23.0	$10\bar{3}$	8.9	− 2.4	$50\bar{5}$	88.7	+ 91.6
204	91.0	− 90.7	$10\bar{5}$	8.0	− 2.4	$60\bar{2}$	5.9	− 1.2
206	31.0	− 19.8	$10\bar{7}$	47.4	− 49.1	$60\bar{4}$	77.0	− 73.8
301	91.9	+ 93.4	$20\bar{2}$	112.9	+115.2	$70\bar{1}$	25.3	− 32.7
303	139.8	+144.4	$20\bar{4}$	71.0	+ 64.4	$70\bar{3}$	36.1	+ 38.2
305	58.8	+ 58.2	$20\bar{6}$	108.0	+101.4			
400	30.7	− 29.8	$30\bar{1}$	5.5	+ 10.3			

TABLE 3—(*continued*)

*hk*0	$\lvert F_o\rvert$	F_c	*hk*0	$\lvert F_o\rvert$	F_c	*hk*0	$\lvert F_o\rvert$	F_c
020	45.6	+ 52.3	280	37.1	+ 33.9	480	6.6	+ 7.6
040	128.4	−149.9	290	57.8	+ 52.4	490	15.1	− 13.6
060	48.9	+ 44.5	2.10.0	66.5	+ 70.5	4.10.0	105.4	+108.3
080	72.0	+ 62.5	2.11.0	61.1	− 60.7	4.11.0	8.2	− 6.6
0.10.0	7.4	+ 6.9	2.12.0	47.1	+ 46.8	4.12.0	6.9	+ 4.1
0.12.0	81.4	+ 84.9	2.13.0	13.3	+ 11.8	4.13.0	<1.8	+ 0.2
0.14.0	35.1	+ 32.5	2.14.0	11.7	+ 11.1	4.14.0	20.0	− 20.8
0.16.0	88.0	− 93.5	2.15.0	59.6	+ 62.6	510	44.9	− 50.5
0.18.0	13.1	+ 12.0	2.16.0	17.6	− 16.7	520	60.7	− 62.9
110	31.1	+ 27.8	2.17.0	46.6	− 53.4	530	70.3	+ 73.4
120	86.3	+ 94.0	310	52.1	− 56.7	540	26.9	+ 25.7
130	29.9	− 24.6	320	60.6	+ 63.4	550	53.0	+ 58.2
140	77.6	− 73.2	330	121.7	+126.6	560	29.9	+ 28.2
150	84.7	+ 78.6	340	62.0	− 54.7	570	9.3	− 2.1
160	74.8	− 72.3	350	83.6	+ 89.5	580	15.3	− 11.0
170	126.5	+123.9	360	50.4	− 49.6	590	35.5	+ 36.4
180	76.6	+ 67.6	370	10.5	+ 7.2	5.10.0	15.6	+ 17.8
190	57.4	− 58.6	380	84.9	+ 86.7	5.11.0	6.8	− 14.4
1.10.0	16.3	− 19.3	390	30.0	+ 27.2	5.12.0	24.0	+ 21.2
1.11.0	17.1	− 10.1	3.10.0	5.9	− 7.7	600	30.2	+ 32.7
1.12.0	47.0	− 45.8	3.11.0	8.9	− 12.1	610	41.2	− 44.3
1.13.0	62.8	+ 67.9	3.12.0	43.3	− 44.1	620	33.2	+ 40.8
1.14.0	28.2	+ 29.8	3.13.0	38.7	− 35.4	630	5.5	− 7.1
1.15.0	24.0	+ 19.0	3.14.0	17.2	+ 12.0	640	10.6	+ 7.8
1.16.0	7.9	+ 6.3	3.15.0	52.8	+ 56.7	650	61.1	+ 62.7
1.17.0	7.8	+ 6.9	3.16.0	5.9	+ 7.6	660	10.0	− 8.2
200	132.3	+140.8	400	46.4	− 48.4	670	38.0	− 35.6
210	116.0	+119.4	410	12.2	+ 7.6	680	8.3	+ 10.3
220	48.4	+ 45.4	420	62.0	+ 65.6	690	39.9	− 43.1
230	26.3	+ 23.3	430	7.5	− 15.5	710	14.0	+ 15.0
240	23.4	− 27.8	440	68.4	+ 64.1	720	39.0	− 53.4
250	87.3	− 78.4	450	3.6	+ 0.7	730	15.2	− 14.6
260	36.5	− 32.1	460	74.1	− 77.2			
270	52.2	+ 55.6	470	13.0	− 5.5			

values for the (200) plane probably is an extinction effect; in any case $|\Delta F|$ for this plane is greater than 5 times the probable error of a single ΔF (calculated for all 95 values of $\Delta F = |F_R| - |F_J|$) and, therefore, it may be rejected. For the other 94 planes, the discrepancy, $\Sigma|F_R - F_J|/\Sigma|F_R|$, between the photometer measurements, F_R, and the eye estimations, F_J, is 0.06_1, in exact agreement with the corresponding value for the 27 reflections of lindgrenite. For the 94 planes of dibenzul, $\overline{\Delta F} = 0.074$, $\Sigma(\Delta F) = 7$, $\Sigma(\Delta F)^2 = 111$, $\sigma(\Delta F) = 1.09$, $\sigma(F) = 0.76_8$, $\sigma(\overline{\Delta F}) = 0.109$. Considering the disparity in the number of available planes involved, these results are not significantly different from those deduced from the lindgrenite data.[3]

[3]The expressions for $\sigma(\Delta F)$ and $\sigma(F)$ are strictly valid only if $|\Delta F|$ is independent of $|F|$. Now the number of observations in the lindgrenite case is rather small (27), and the range of $|F|$ is not large ($\sim$7 to $\sim$36), but the mean $|\Delta F|$'s calculated for separate groups

The structure factors (F_c) in Table 3 have been calculated with the atomic co-ordinates shown separately for each zone in Table 1. The final values of R, obtained directly from the data in Table 3, are 0.07 for the $\{0kl\}$ zone, 0.07 for the $\{h0l\}$ zone, and 0.09 for the $\{hk0\}$ zone when all planes are included; if the planes (040) and (720) are excluded, because $|\Delta F|$ for each (where $\Delta F = |F_o| - |F_c|$) is greater than 5 times the P.E. of a single ΔF, and the unobserved (4.13.0) is ignored, R for the $\{hk0\}$ zone is 0.08.

Because of the inherent difficulty of locating the oxygen atoms with reasonable accuracy in the presence of the much heavier atoms of copper and molybdenum in lindgrenite, special care was taken throughout this investigation to reduce errors of observation to a minimum. Intensity estimations, whether by photometer or by eye, were made several times for each reflection, the use of the spherical crystal removed much uncertainty in the corrections for absorption, and, by recourse to very long exposure times, 268 of a possible 270 reflections were observed, although 18 observed (and 1 of the unobserved) reflections, for which $\sin\theta$ was large, were rejected because of uncertainty in the evaluation of their Lorentz-polarization factors. Errors due to finite series summations were effectively corrected by the use of the difference synthesis method of refinement, and rounding-off errors in the full difference syntheses were reduced by scaling up the coefficients. Taking the estimated $\sigma(F) = |F_o - F_c|$, the values of $\sigma(\rho)$, (Cruickshank, 1949, equation 11.10), in the final Fourier syntheses (Fig. 4) are 1.0 *e.* Å^{-2} for the $\{0kl\}$ zone, 1.8 *e.* Å^{-2} for the $\{h0l\}$ zone, and 0.8 *e.* Å^{-2} for the $\{hk0\}$ zone.

For those atoms which are resolved in projection, the standard

of the larger and the smaller values of $|F|$ do suggest that $|\Delta F|$ probably is not independent of the magnitude of the structure amplitude. In the case of dibenzyl (94 planes), the mean $|\Delta F|$ is 1.64 for the largest amplitudes ($70 \geqslant |F_R| \geqslant 20$; 11 planes), it is 0.76 for the middle group ($20 > |F_R| \geqslant 10$; 33 planes), and it is 0.48 for the smallest amplitudes ($10 > |F_R| \geqslant 2$; 50 planes). Also, the discrepancy between F_R and F_J (0.06_1 for all planes) is 0.04_6 for the first, 0.05_7 for the second, and 0.08_6 for the third of these groups. Because of the scarcity of available data suitable for direct comparison of photometered and eye-estimated intensities, it is of interest to summarize other forms in which the dibenzyl results have been expressed, particularly in view of the fact that they are not all mutually consistent for reasons that are not immediately apparent. There seems to be no doubt that the 94 pairs of F's (R & J) from Jeffrey's Table 1 (Jeffrey, 1947, p. 224), for which observed values are given (omitting the (200) plane), have been used in all cases. Jeffrey (1947) has shown that the differences between the R and J results (even when the (200) plane is included) "form an approximately normal error curve from which the most probable error is 0.6". Cruickshank (1949, p. 73) gives the standard deviation for all planes as 1.12 (omitting the (200) plane), and points out that this must be divided by $\sqrt{2}$ because both sets of observations are subject to error; thus, $1.12/\sqrt{2} = 0.79_2$. Lipson & Cochran (1953, p. 289) express this as "$\sigma(F_o) = 0.8$, assuming $\sigma(F_o)$ independent of $|F_o|$". Finally, Jeffrey & Cruickshank (1953, p. 367) state that, "In dibenzyl, for 94 reflections the s.d. of the difference between independent measurements by photometer and by visual estimation was 5.0% of the mean $|F^{obs.}|$."

TABLE 4. STANDARD DEVIATIONS (in Å) OF ATOMIC CO-ORDINATES
(Separately for Each Zone; Standard Deviations of Weighted Means, s.d.w.m.)

Atom	x			y			z		
	$\{h0l\}$	$\{hk0\}$	s.d.w.m.	$\{0kl\}$	$\{hk0\}$	s.d.w.m.	$\{0kl\}$	$\{h0l\}$	s.d.w.m.
Cu_1	0	0	0	0	0	0	0	0	0
Cu_2	(0.01)	0.004	0.004	0.004	0.003	0.002	0.004	0.005	0.003
Mo	0.003	0.002	0.002	0.002	0.002	0.001	0.003	0.003	0.002
O_1	(0.04)	0.01	0.01	0.009	0.006	0.01	0.03	(0.04)	0.03
O_2	(0.04)	(0.02)	0.02	(0.02)	(0.02)	0.01	(0.02)	(0.04)	0.02
O_3	(0.03)	(0.02)	0.02	(0.03)	0.02	0.02	(0.03)	(0.04)	0.02
O_4	(0.02)	0.01	0.01	(0.02)	(0.04)	0.04	0.02	0.01	0.02
OH	0.009	0.009	0.01	0.01	0.01	0.01	0.01	0.005	0.01

deviations of individual co-ordinates have been calculated with the aid of Cruickshank's formula 11.12 (Cruickshank, 1949, p. 72). For those atoms which are not resolved, the standard deviations of the co-ordinates have been estimated with the aid of the approximation given by Lipson & Cochran (1953, p. 279, equation 279.4) for the electron density near the centre of an atom, peak curvatures being obtained from the partial difference maps (Fig. 2). All results are shown in Table 4, where the values in parentheses are those for atoms which are not fully resolved. The standard deviations of the weighted mean co-ordinates (see Table 1) also are included in Table 4; their r.m.s. values are as follows: Mo, 0.002 Å; Cu, 0.003 Å; O_1, O_2, O_3, O_4, none of which is fully resolved in all three projections, 0.02 to 0.03 Å; OH (fully resolved), 0.01 Å. The standard deviations for the metal-oxygen and metal-hydroxyl distances are virtually the same as those for the O and OH co-ordinates because the s.d. of the latter are so much greater than the s.d. of the metal co-ordinates. The standard deviation of the Mo–Cu distances is 0.004 Å. The probable errors in the unit cell constants of lindgrenite have no significant effect on the standard deviations of the interatomic distances.

Description and Discussion

Axial projections of the structure of lindgrenite are shown in Figs. 5, 6, 7. The explanation of the perfect cleavage parallel to (010) is immediately apparent from an inspection of Figs. 5 and 7.

In lindgrenite each atom of molybdenum is surrounded by four atoms of oxygen (O_1, O_2, O_3, O_4) at the corners of an essentially regular tetrahedron (see Table 2) in which the average length of the Mo–O bond is 1.74 Å, the average O—O distance is 2.84 Å, and the average value of the tetrahedral angle is 109.5°. Although the co-ordination of O around Mo in molybdenum compounds frequently is octahedral, it is both tetrahedral and octahedral in Mo_4O_{11} (Magnéli, 1948) where the Mo—O

bond length in the tetrahedra is 1.75 Å. Donohue & Shand (1947) report 1.83 Å for the length of the Mo—O bond in the regular MoO_4 tetrahedra of Ag_2MoO_4. There appears to be nothing unusual, therefore, about the MoO_4 tetrahedra in lindgrenite.

Two crystallographically distinct oxy-hydroxy octahedra are co-ordinated around the copper atoms (Cu_1) at the symmetry centres and those (Cu_2) in general positions. Both Cu_1 and Cu_2 have two O and two OH as nearest neighbours in approximately square array with two O (one above and one below the plane of the square) on the normal through the Cu at the centre. In both octahedra the Cu—O bonds normal to the square are appreciably longer (averages: 2.46 Å for Cu_1, 2.42 Å for Cu_2) than the Cu—O, Cu—OH bonds in the plane of the square (averages: 1.97 Å for Cu_1, 1.95 Å for Cu_2). The octahedron around Cu_1 is

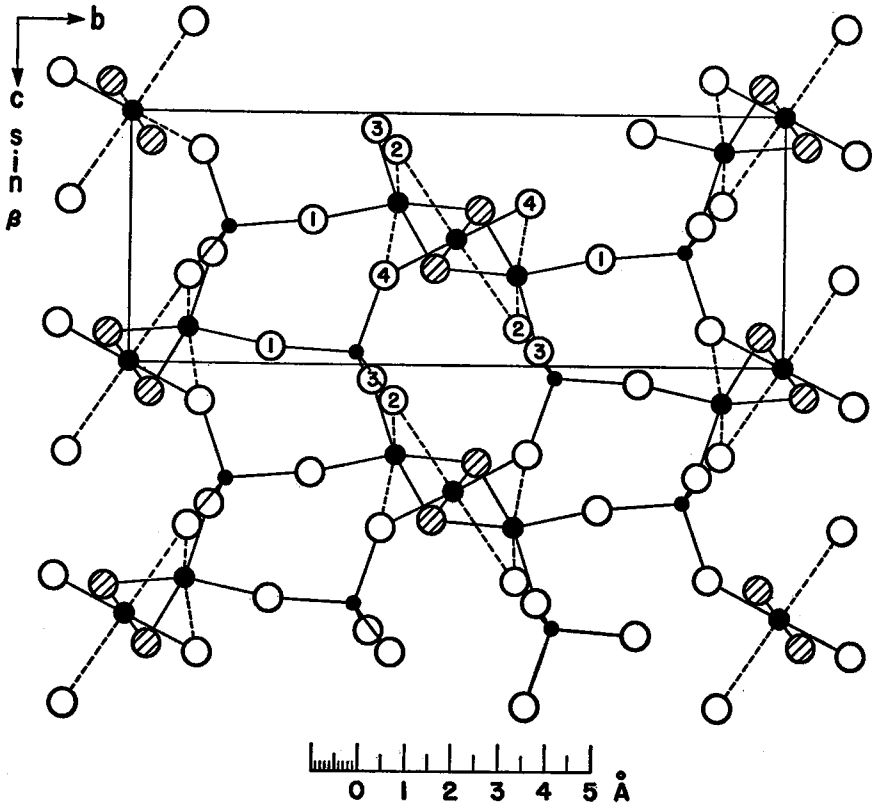

FIG. 5. Projection of the structure of lindgrenite on (100). One unit cell outlined; large solid circles, Cu; small solid circles, Mo; open numbered circles, O_1, O_2, O_3, O_4; hatched circles, OH.

much less distorted than the one around Cu_2. The two OH are diagonally situated in the O_4—OH—O_4—OH square having Cu_1 at the approximate centre, but they are adjacent in the O_1—OH—OH—O_3 square around Cu_2. Furthermore, each Cu_1-octahedron shares four edges (two O_4—OH, two OH—O_2) with four neighbouring Cu_2-octahedra, whereas each Cu_2-octahedron shares two edges (O_4—OH, OH—O_2) with two adjacent Cu_1-octahedra and one edge (OH—OH) with an adjacent Cu_2-octahedron. The interactomic distances along shared edges (designated by an asterisk in Table 2) are significantly shorter than those along corresponding edges that are not shared. Also, the very short OH—OH edge (2.53 Å) which is shared between two Cu_2-octahedra is associated with a relatively short Cu_2—Cu_2 distance of 3.01 Å; the other distances between copper atoms are 3.15 Å and 3.22 Å, between Cu_2 in one octahedron and Cu_1 in two adjacent octahedra.

The $CuO_4(OH)_2$ octahedra share 4 and 3 edges alternately to form

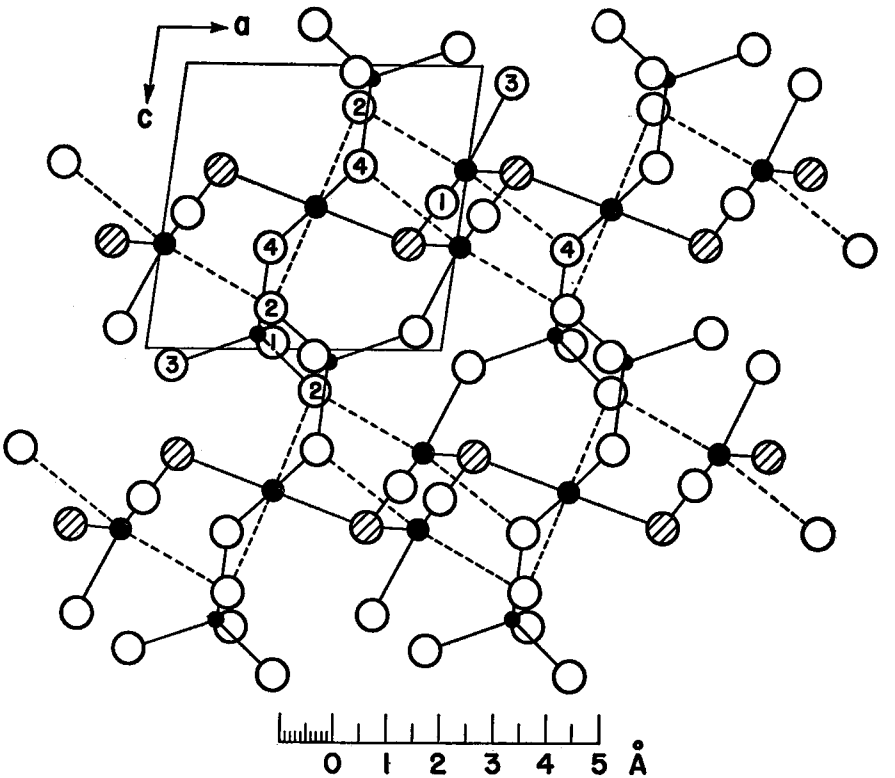

FIG. 6. Projection of the structure of lindgrenite on (010). Symbols as in Fig. 5. Only the metal atoms between $\frac{1}{4}b$ and $\frac{3}{4}b$, with their associated O and OH, are shown.

endless chains. These chains are cross-linked through the MoO_4 tetrahedra to form an infinite three-dimensional network. Each MoO_4 tetrahedron shares its four corners as follows: O_1 with a Cu_2-octahedron; O_2 with both a Cu_1-octahedron and a Cu_2-octahedron; O_3 with a Cu_2-octahedron; and O_4 with both a Cu_1-octahedron and a Cu_2-octahedron; but not all of these octahedra are parts of the same chain. The corresponding Mo—Cu distances are Mo—Cu_2, 3.63 Å; Mo—Cu_1, 3.65 Å and Mo—Cu_2, 3.91 Å; Mo–Cu_2, 3.42 Å; Mo—Cu_1, 3.42 Å and Mo—Cu_2, 3.70 Å. Since the tetrahedra are essentially regular, the variations among the Mo—Cu distances (particularly those for Mo—Cu_2) illustrate the distortion of the octahedra, especially that around Cu_2.

A portion of one of the chains of $CuO_4(OH)_2$ octahedra, with four of the MoO_4 tetrahedra, is shown in idealized form in Fig. 8.

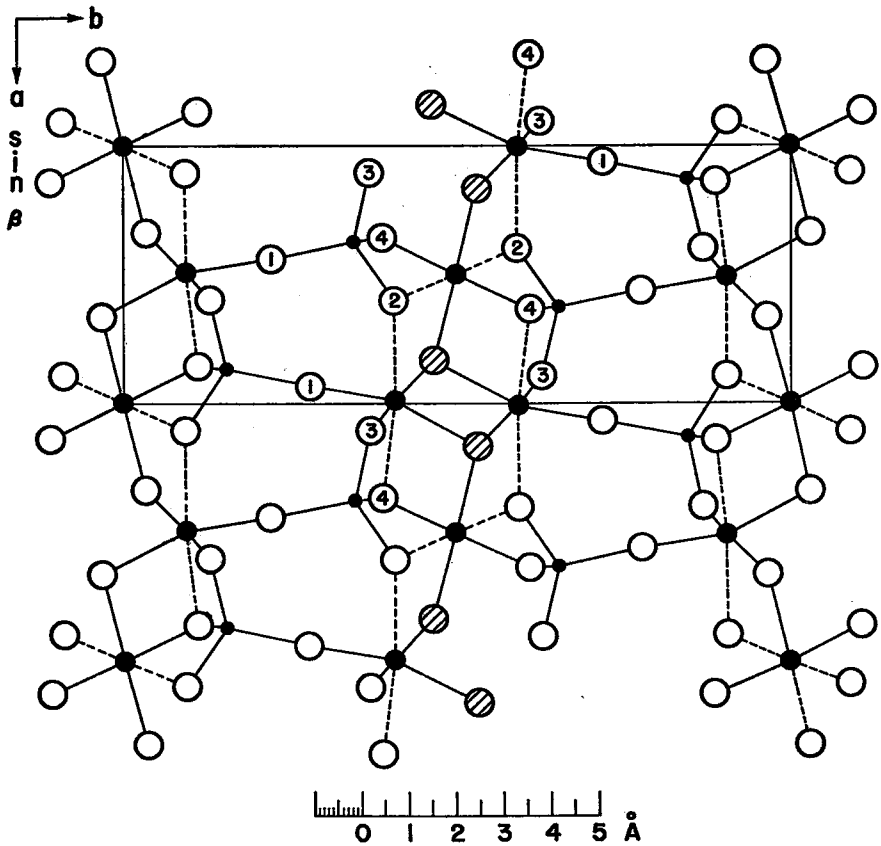

FIG. 7. Projection of the structure of lindgrenite on (001). Symbols as in Fig. 5.

It is of interest to compare the $CuO_4(OH)_2$ octahedra of lindgrenite, a basic copper molybdate, with the $CuO_4(OH)_2$ and $CuO_2(OH)_4$ octahedra of malachite, a basic copper carbonate (Wells, 1951). In malachite, Cu_I is at the centre of a square (O—OH—O—OH) in which the average Cu—O, Cu—OH bond length is 1.98 Å, and two oxygen atoms are situated on the normal to the square, one above and one below, at an average Cu—O distance of 2.71 Å. A similar square (O—OH—O—OH), in which the average Cu—O, Cu—OH bond length is 2.01 Å, surrounds

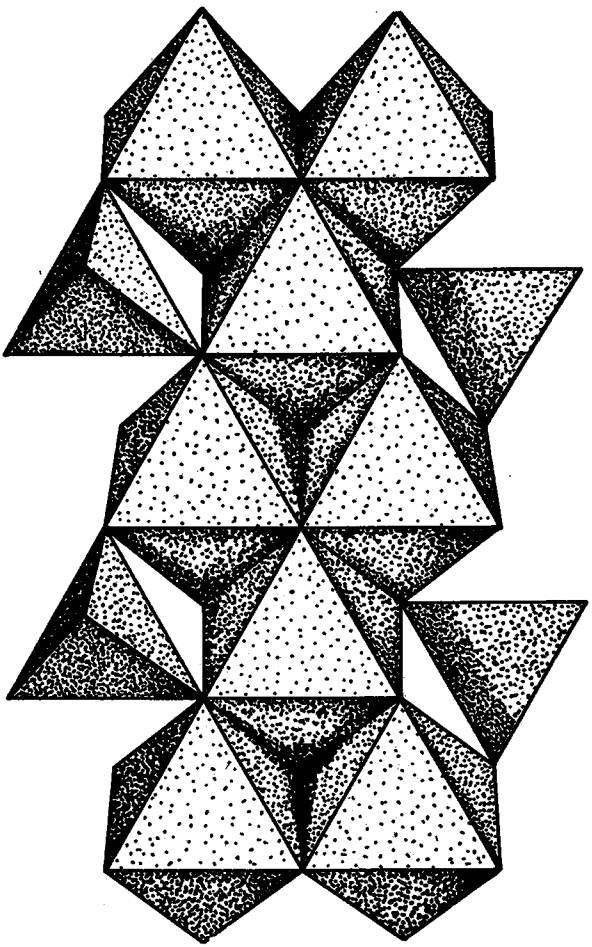

FIG. 8. An idealized portion of one of the endless chains of $CuO_4(OH)_2$ octahedra in lindgrenite with four of the MoO_4 tetrahedra through which the chains are cross-linked to form an infinite three-dimensional network. Each of the two octahedra on the vertical central line is co-ordinated around a copper atom (Cu_I) at a center of symmetry.

Cu_{II} but, in this octahedron, hydroxyl groups are located on the normal to the plane of the square at an average Cu—OH distance of 2.41 Å. Thus in both Cu-octahedra of malachite the two OH in the square are across a diagonal as in the Cu_1-octahedron of lindgrenite. Furthermore, there are no significant differences among the average Cu—O, Cu—OH bond lengths within the squares around Cu_1 and Cu_2 in lindgrenite, and Cu_I and Cu_{II} in malachite. All four octahedra are elongated along the normal to the plane of the square, and the Cu_1—O and Cu_2—O bond lengths along this normal in lindgrenite are virtually the same as the corresponding Cu_{II}—OH bond length in malachite, but they are significantly shorter than the length of the Cu_I—O bond in the other malachite octahedron.

Grateful acknowledgment is made to Mrs. M. E. Pippy for carrying out many of the calculations, and to Mrs. H. M. Sheppard and Mr. B. J. Cowick for assistance in collecting the powder data.

References

BARNES, W. H. (1949): (*a*) The unit cell and space group of lindgrenite, *Am. Mineral.*, **34**, 163–172; (*b*) Some comments on the Buerger precession method for the determination of unit cell constants and space groups, *ibid*, 173–180; (*c*) Corrections to recent papers on probertite and lindgrenite, *ibid*, 611–612.

BOND, W. L. (1951): Making small spheres, *Rev. Sci. Instr.*, **22**, 344–345. (The equipment in this laboratory consists of a Bond Sphere Grinder, Model 440, Lovins Engineering Co., Silver Springs, Md., and a Type HB Air Transformer, DeVilbiss Mfg. Co., Windsor, Ont., on a compressed air line).

BUERGER, M. J. (1941): *Numerical structure factor tables*, (Geol. Soc. America Special Paper **33**).

CANNON, R. S. & GRIMALDI, F. S. (1953): Lindgrenite and cuprotungstite from the Seven Devils district, Idaho, *Am. Mineral.*, **38**, 903–911.

CRUICKSHANK, D. W. J. (1949): The accuracy of electron-density maps in *x*-ray analysis with special reference to dibenzyl, *Acta Cryst.*, **2**, 65–82.

DONOHUE, J. & SHAND, W. (1947): The determination of the interatomic distances in silver molybdate, Ag_2MoO_4, *J. Am. Chem. Soc.*, **69**, 222–3.

EVANS, H. T. & EKSTEIN, M. G. (1952): Tables of absorption factors for spherical crystals, *Acta Cryst.*, **5**, 540–542.

HÖNL, H. (1933): Atomfaktor für Röntgenstrahlen als Problem der Dispersionstheorie (K-Schale), *Ann. d. Physik*, **18**, 625–655.

Internationale Tabellen zur Bestimmung von Kristallstrukturen (1935), Borntraeger, Berlin.

JEFFREY, G. A. (1947): The structure of polyisoprenes. VI. An investigation of the molecular structure of dibenzyl by *x*-ray analysis. *Proc. Roy. Soc.*, **A188**, 222–233.

JEFFREY, G. A. & CRUICKSHANK, D. W. J. (1953): Molecular structure determination by *x*-ray crystal analysis: modern methods and their accuracy, *Quart. Rev. Chem. Soc., Lond.*, **7**, 335–376.

KINGSBURY, A. W. G. & HARTLEY, J. (1954): On the occurrence of the rare copper molybdate, lindgrenite, at Brandy Gill, Carrock Fell, Cumberland, *Am. Mineral.*, **39**, 842.

LIPSON, H. & COCHRAN, W. (1953): *The determination of crystal structures*, Bell, London.

MAGNÉLI, A. (1948): The crystal structure of Mo_4O_{11} (γ-molybdenum oxide), *Acta Chem. Scand.*, **2**, 861–871.

PALACHE, C. (1935): Lindgrenite, a new mineral, *Am. Mineral.*, **20**, 484–491.
ROBERTSON, J. M. (1934): *X*-ray analysis of the crystal structure of dibenzyl. I. Experimental and structure by trial. *Proc. Roy. Soc.*, **A146**, 473–482.
SCARBOROUGH, J. B. (1950): *Numerical mathematical analysis*, Johns Hopkins, Baltimore.
TAYLOR, A. (1944): The influence of crystal size on the absorption factor as applied to Debye-Scherrer diffraction patterns, *Phil. Mag.*, **35**, 215–229 (for spherical crystals, see pp. 218, 227).
WASER, J. (1951): Lorentz and polarization correction for the Buerger precession method, *Rev. Sci. Instr.*, **22**, 567–568.
WEATHERBURN, C. E. (1947): *Mathematical statistics*, Cambridge, p. 170.
WELLS, A. F. (1951): Malachite, re-examination of crystal structure, *Acta Cryst.*, **4**, 200–204.
WIEBENGA, E. H. & SMITS, D. W. (1950): An integrating Weissenberg apparatus for *x*-ray analysis, *Acta Cryst.*, **3**, 265–267.
WILSON, A. J. C. (1942): Determination of absolute from relative *x*-ray intensity data, *Nature*, **150**, 152.
YOUDEN, W. J. (1951): *Statistical methods for chemists*, Wiley, New York.

APPENDIX

X-RAY DIFFRACTION POWDER DATA FOR LINDGRENITE

(Cu$K\alpha$, λ = 1.5418 Å; camera radius, 114.6 mm.; cut-off, 17 Å; Straumanis film mounting; negligible film shrinkage; indexed on basis of $a = 5.61_3$, $b = 14.03$, $c = 5.40_5$ Å, $\beta = 98°23'$, $P2_1/n$; I/I_1 estimated by eye with aid of intensity scale; B (or BB) indicates a broad (or very broad) line)

I/I_1	d(Å) Obs.	d(Å) Calc.	*hkl*	I/I_1	d(Å) Obs.	d(Å) Calc.	*hkl*	I/I_1	d(Å) Obs.
20	7.01	7.02	020	20	2.46	2.46	$22\bar{1}$	5	1.40
5	5.15	5.16	110	20	2.40	2.40	$12\bar{2}$	15	1.39
5	4.97	5.00	011			2.39	230	10	1.37
35	4.34	4.35	120			2.34	060	5B	1.34
—	—	4.25	021	—	—	2.33	$15\bar{1}$	8	1.29
55	4.15	4.17	$10\bar{1}$			2.32	032	5	1.27
—	—	3.99	$11\bar{1}$			2.30	211	8B	1.25
25	3.58	3.60	101	25	2.29	2.29	$23\bar{1}$	1	1.23
		3.58	130, $12\bar{1}$	1	2.25	2.25	112, $13\bar{2}$	2B	1.20
100	3.50	3.52	031	15	2.21			2B	1.16
		3.51	040	10	2.15			2B	1.15
25	3.47	3.49	111	5B	2.08			2	1.13
10	3.19	3.20	121	10	1.97			1	1.104
10	3.11	3.11	$13\bar{1}$	20	1.93			2	1.097
20	2.96	2.97	140	20	1.90			2	1.054
10	2.92	2.93	041	25	1.88			2	1.039
15	2.84	2.85	131	10	1.78			1	1.019
20	2.76	2.78	200	15	1.76			1	1.011
20	2.72	2.72	210	25	1.72			3	0.988
40	2.67	2.68	$14\bar{1}$	20B	1.66			1	0.977
		2.67	002	20	1.59			1	0.969
2	2.62	2.63	012	10BB	1.57			2	0.959
2	2.57	2.58	220, $21\bar{1}$	2	1.54			1B	0.932
—	—	2.52	$11\bar{2}$	2	1.52			1B	0.904
25	2.50	2.51	141	10	1.49			1	0.884
		2.50	022, 150	1	1.46			1	0.871
		2.48	051	10	1.44				